Supplementary Materials

Understanding the variation of Reflected Solar Radiation: A Latitude- and month-based Perspective

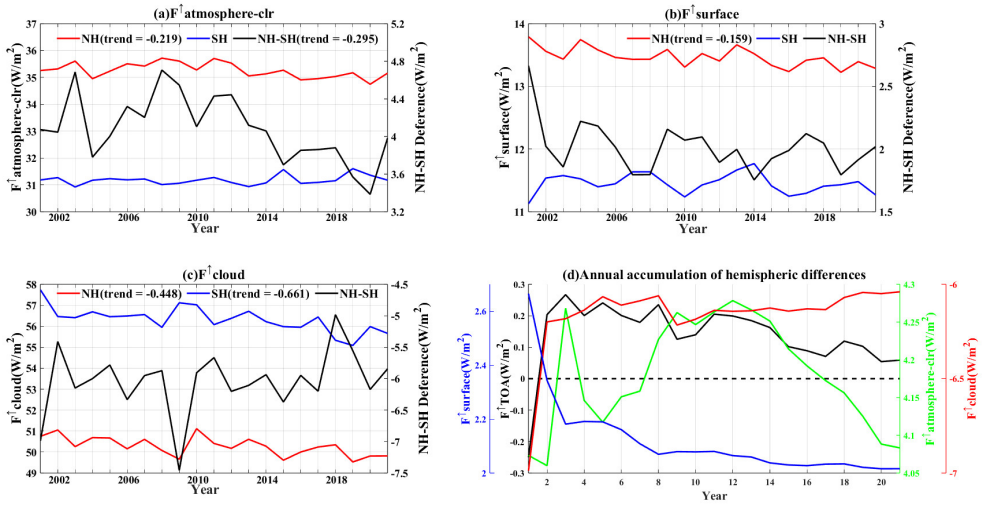

Figure S1: Interannual variability of (a) the clear-sky atmospheric component, (b) the surface component, and (c) the cloud component for the NH and SH, 2001-2021. The red line represents the NH, the blue line represents the SH and corresponds to the left y-axis, and the black line represents the difference between the two hemispheres and corresponds to the right y-axis. The trends labeled pass the 99% significance test in units of W m^{-2} $(10a)^{-1}$). Note that the trend in the clear-sky atmospheric component of the NH labeled in (a) only passes the 95% significance test. Unlabeled trends do not pass the test of significance. (d) Cumulative annual mean for hemispheric differences of radiative fluxes. That is, when Year=N (1≤N≤21), interhemispheric differences (NH-SH) of annual mean radiative fluxes are calculated from 2001 to 200+(N-1). The black color indicates the hemispheric difference of the total reflected radiative flux at the TOA, while the blue, green, and red colors correspond to the hemispheric differences of the three components, respectively.

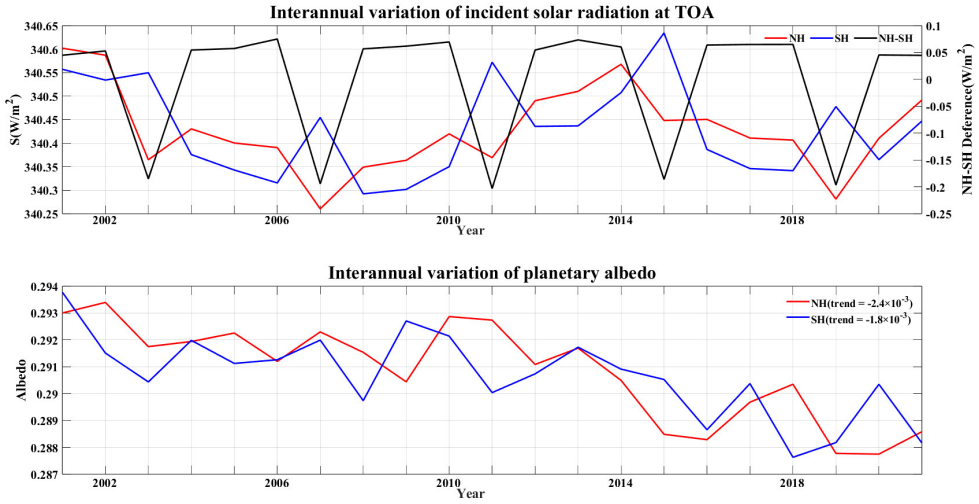

Figure S2: Interannual variability of (a) TOA incident solar radiation flux and (b) planetary albedo for the NH and SH, 2001-2021. The red line represents the NH, the blue line represents the SH and corresponds to the left y-axis, and the black line in the diagram above represents the difference between the NH and SH and corresponds to the right y-axis. The trends labeled passes the 99% significance test in units of $(10a)^{-1}$.

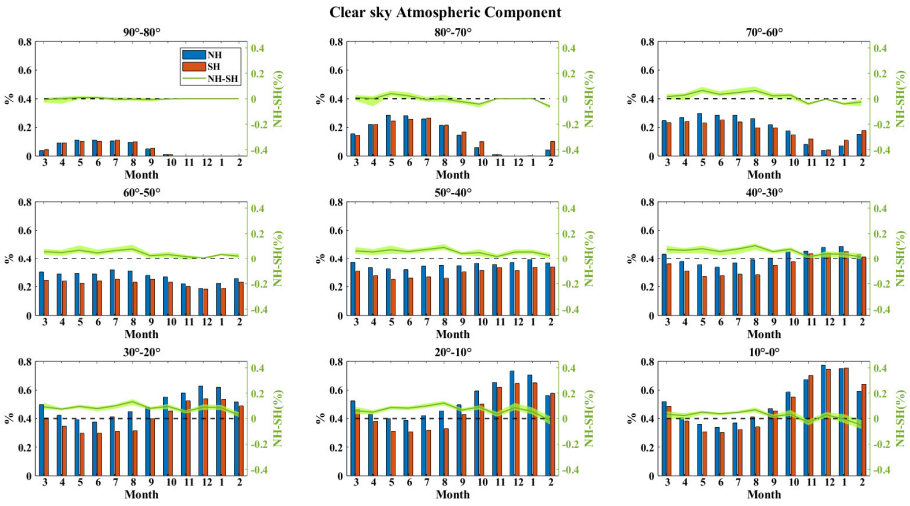

Figure S3: Same as Fig. 3, but for the clear-sky atmospheric component.

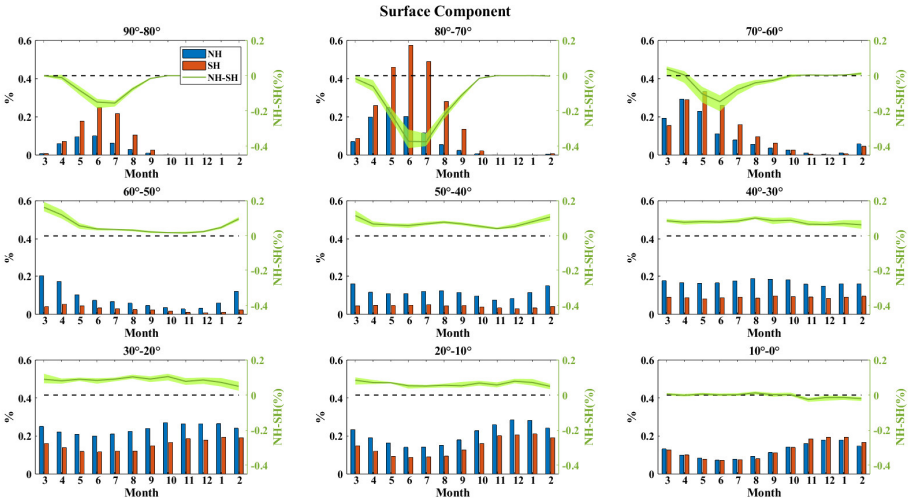

Figure S4: same as Fig. 3, but for surface component.

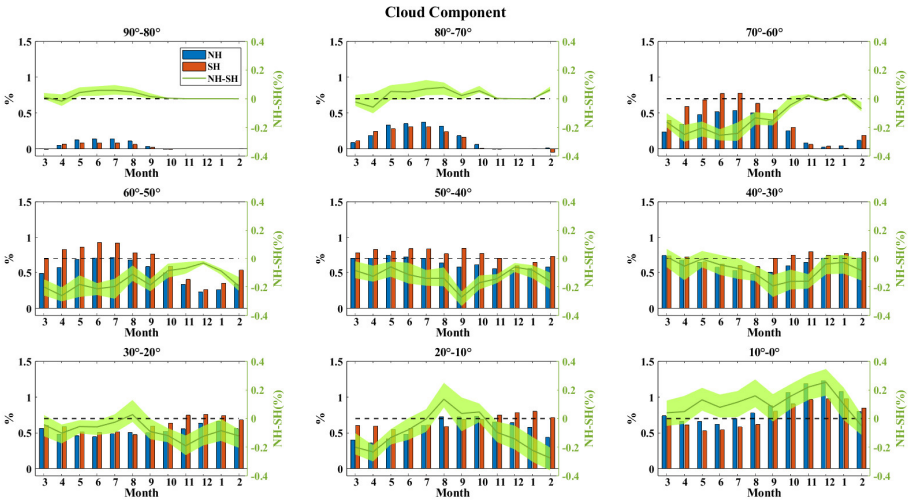

Figure S5: same as Fig. 3, but for cloud component.

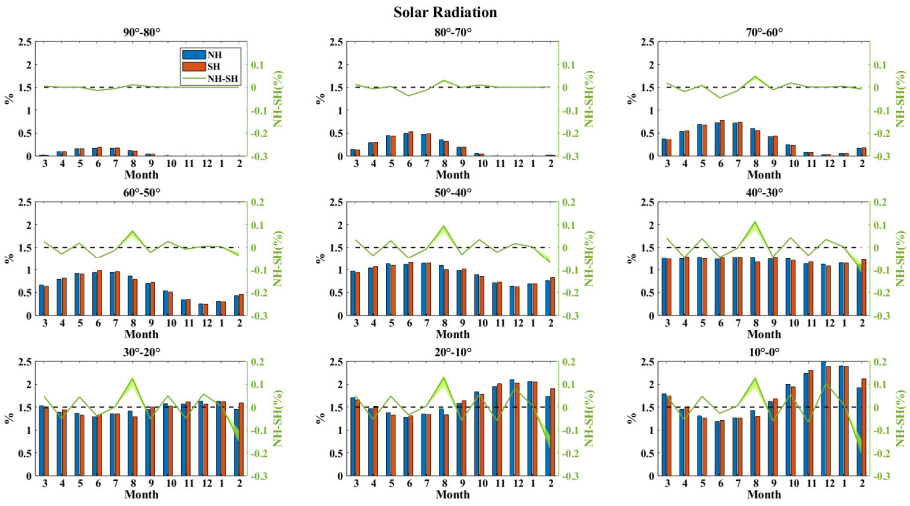

Figure S6: same as Fig. 3, but for incident solar radiation at the TOA.

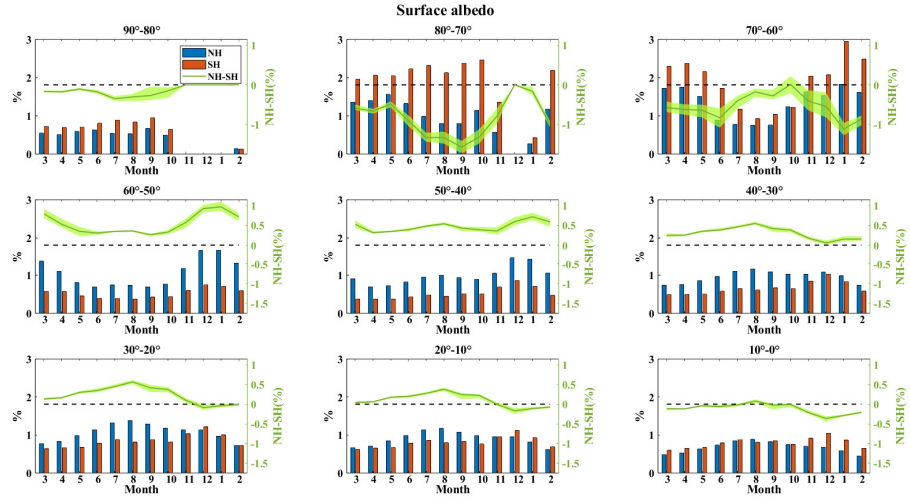

Figure S7: same as Fig. 3, but for surface albedo.

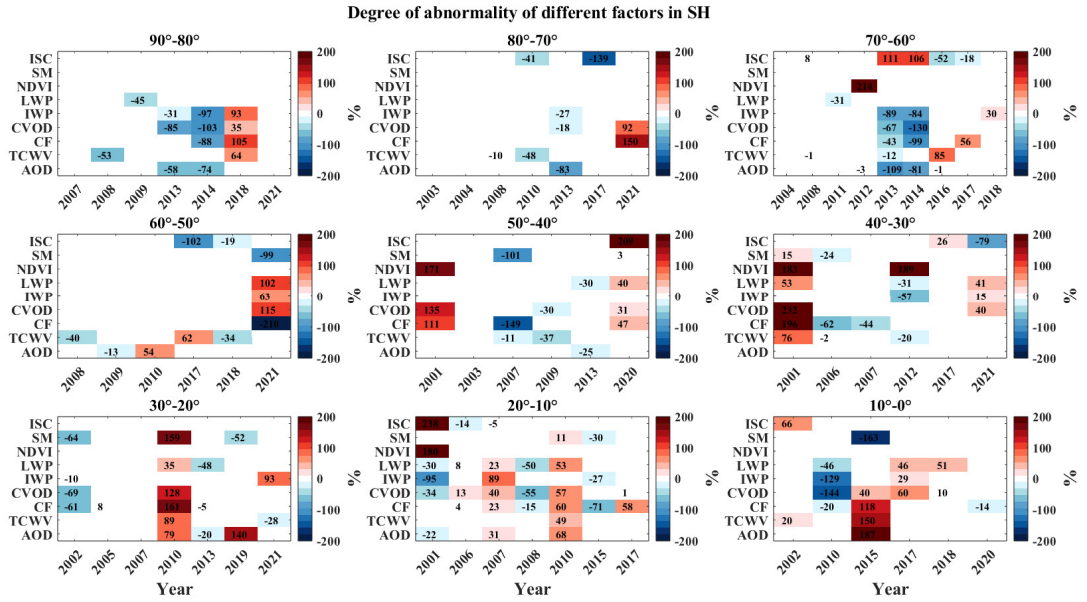

Figure S8: The degree of anomalies of the different factors that were outside their normal ranges (one standard deviation) in extreme anomalous years of different latitudinal zones in SH.

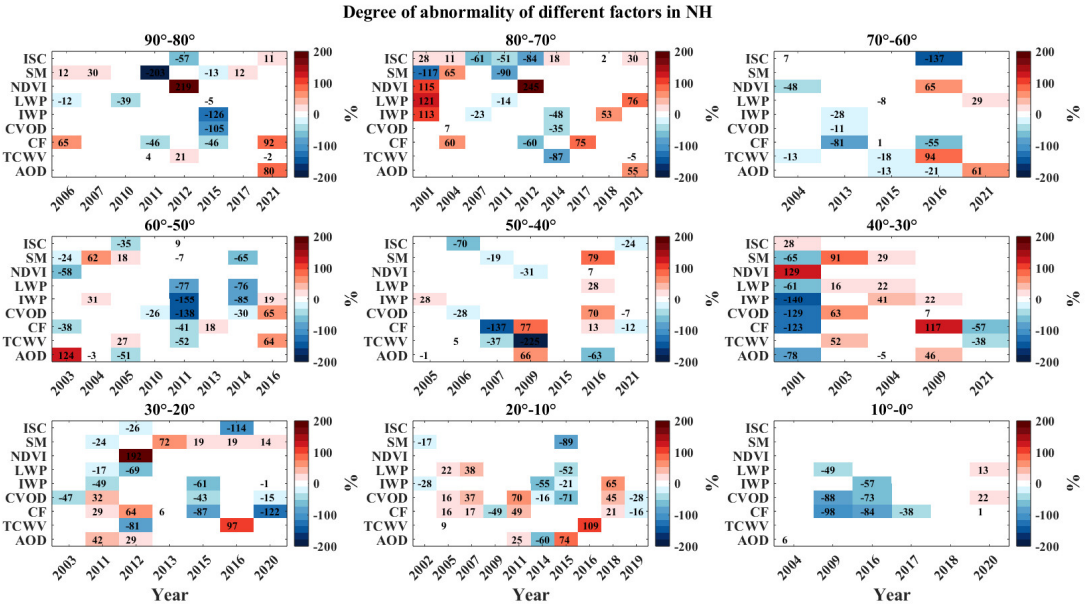

Figure S9: The degree of anomalies of the different factors that were outside their normal ranges (one standard deviation) in extreme anomalous years of different latitudinal zones in NH.

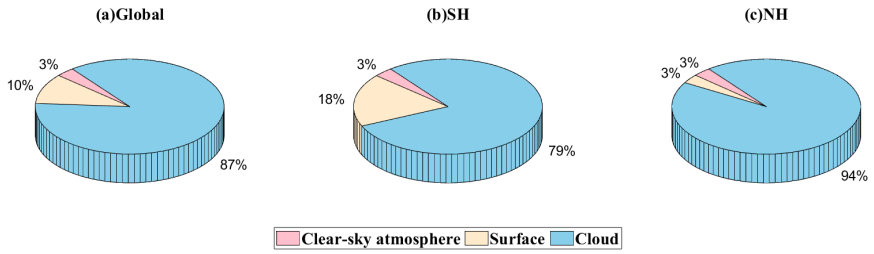

Figure S10: The proportion of the largest contribution anomalies of three component in extreme anomalous years of (a) global, (b) SH and (c) NH. Pink, yellow, and blue colors indicate the proportion of extreme anomaly years dominated by clear-sky atmospheric component contribution anomalies, surface component contribution anomalies, and cloud component contribution anomalies, respectively.

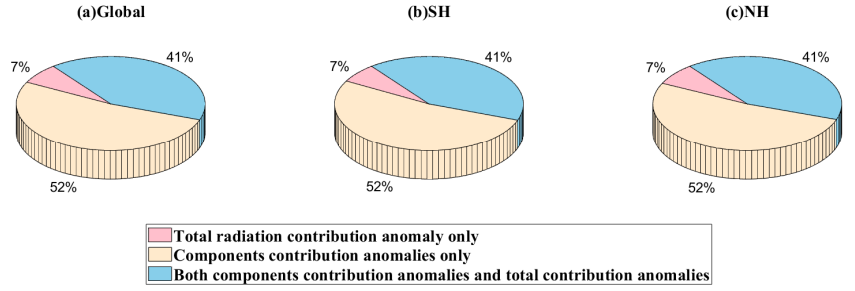

Figure S11: Proportion of different situations for all events in (a) global, (b) SH and (c) NH with extreme values (extreme values of total radiative contribution anomalies or extreme values of component contribution anomalies). Pink, yellow and blue colors indicate that only the total radiation contribution anomaly is extreme, only the component contribution anomaly is extreme and not only the component contribution anomaly is extreme but also the total radiation contribution anomaly, respectively.

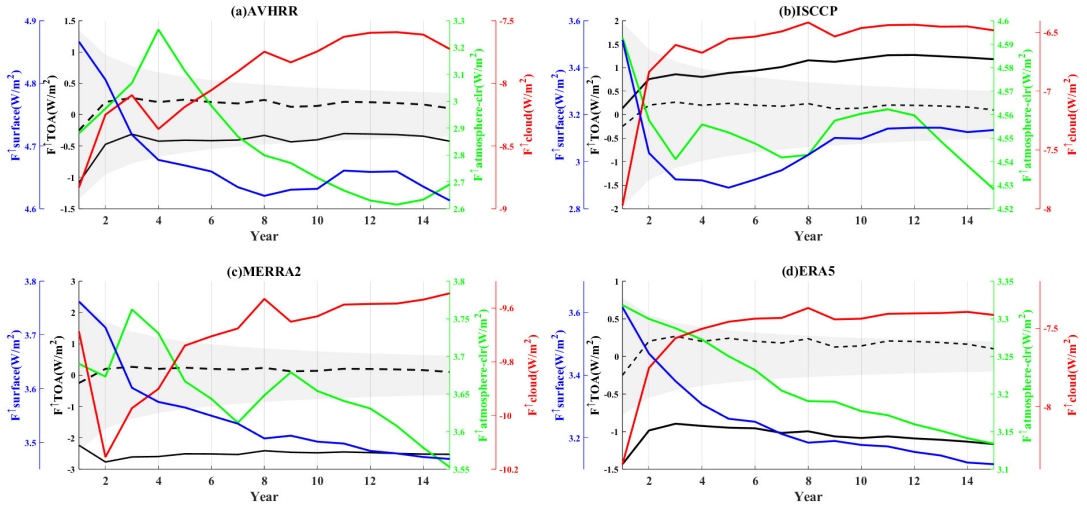

Figure S12: Cumulative annual mean for hemispheric differences of radiative fluxes. Same as the (d)-subplot of Fig.S1, but for (a) AVHRR, (b) ISCCP, (c) MERRA-2 and (d) ERA5. Note that the black dashed line shows the accumulation of hemispheric differences in the total reflected radiative flux at the TOA for CERES-EBAF. The shaded areas in (a)-(d) are the uncertainties of hemispheric difference of TOA reflected SW flux for AVHRR, ISCCP, MERRA-2 and ERA5, respectively. If the solid black line is within the shaded area, it indicates that the hemispheric difference in total reflected radiation is credible within the uncertainty.

Table S1: CCHZ-DISO system with different calculation indicators

(a) Interannual hemispheric asymmetry

Datasets	Time-CC	NAE	NRMSE	DISO
CERES	1	0	0	0
AVHRR	0.96	0.14	0.21	0.25
ISCCP	0.71	-0.29	0.43	0.59
MERRA-2	0.32	0.71	1	1.40
ERA5	0.84	0.34	0.48	0.61

(b) Interannual hemispheric asymmetry

Datasets	Time-CC	STD	Centered-RMS	DISO
CERES	1	0.45	0	0
AVHRR	0.96	0.57	0.18	0.22
ISCCP	0.71	0.52	0.37	0.48
MERRA-2	0.32	0.38	0.49	0.84
ERA5	0.84	0.32	0.25	0.33

(c) Interannual hemispheric asymmetry

Datasets	Time-CC	NAE	NRMSE	Space-CC	DISO
CERES	1	0	0	1	0
AVHRR	0.96	0.14	0.21	0.97	0.26
ISCCP	0.71	-0.29	0.43	0.96	0.59
MERRA-2	0.32	0.71	1	0.79	1.42
ERA5	0.84	0.34	0.48	0.92	0.62